In situ Hydrogels Prepared by Photo-initiated Crosslinking of Acrylated Polymers for Local Delivery of Antitumor Drugs

Yuandou Wang, Shuxin Wang, Wenju Hu, Shaowen Kong, Feng Su, Fusheng Liu, Suming Li

In situ Hydrogels Prepared by Photo-initiated Crosslinking of Acrylated Polymers for Local Delivery of Antitumor Drugs

Yuandou Wang[a,b], Shuxin Wang[a,b], Wenju Hu[a,b], Shaowen Kong[a,b], Feng Su[a,b,*], Fusheng Liu[a,*], Suming Li[c,*]

[a] *College of Chemical Engineering, Qingdao University of Science and Technology, Qingdao 266042, China*
[b] *Institute of High Performance Polymers, Qingdao University of Science and Technology, Qingdao 266042, China*
[c] *Institut Européen des Membranes, IEM UMR 5635, Univ Montpellier, CNRS, ENSCM, Montpellier, France*

A triblock copolymer was synthesized by ring opening polymerization of ε−caprolactone in the presence of poly(ethylene glycol) (PEG). The resulted PCL-PEG-PCL triblock copolymer, PEG and monomethoxy (MPEG) were functionalized by end group acrylation. NMR and FT-IR analyses evidenced the successful synthesis and functionalization of polymers. A series of photo-crosslinked hydrogels composed of acrylated PEG-PCL-Acr and MPEG-Acr or PEG-Acr were prepared by exposure to visible light using lithium phenyl-2,4,6-trimethylbenzoylphosphinate as initiator. The hydrogels present a porous and interconnected structure as shown by SEM. The swelling performance of hydrogels is closely related to the crosslinking density and hydrophilic content. Addition of MPEG or PEG results in increase in water absorption capacity of hydrogels. In vitro degradation of hydrogels was realized in the presence of a lipase from porcine pancreas. Various degradation rates were obtained which mainly depend on the hydrogel composition. MTT assay confirmed the good biocompatibility of hydrogels. Importantly, in situ gelation was achieved by irradiation of a precursor solution injected in the abdomen of mice. Doxorubicin (DOX) was selected as a model antitumor drug to evaluate the potential of hydrogels in cancer therapy. Drug-loaded hydrogels were prepared by in situ encapsulation. In vitro drug release studies showed a sustained release during 28 days with small burst release. DOX-loaded hydrogels exhibit antitumor activity against A529 lung cancer cells comparable to free drug, suggesting that injectable in situ hydrogel with tunable properties could be most promising for local drug delivery in cancer therapy.

Introduction

Hydrogel is a three-dimensional network composed of hydrophilic polymers crosslinked by physical or chemical bonding as first reported by Wichterle and Lim in 1960.[1] Due to their good biocompatibility and physical characteristics such as superabsorbency, viscoelasticity, softness and flexibility, hydrogels have been extensively studied as promising biomaterials for biomedical applications, such as drug or bioactive factor carrier in disease treatment, cell scaffold in tissue engineering, and wound dressing to protect and promote wound healing, etc.[2-5]

Traditional hydrogels are pre-formed and implanted via invasive surgical incision. Nowadays, advances in materials chemistry have made it possible to design and develop injectable in situ-forming hydrogels.[6] Injectable hydrogels can be implanted into the body via a syringe or catheter, greatly reducing surgical costs, improving patient comfort, and enabling minimally invasive treatment.[7] Drugs and bioactive agents can be blended with the hydrogel precursor solution to easily achieve uniform encapsulation in the hydrogel.[8] Moreover, precursor solutions injected in liquid form avoid the shear thinning effect of syringe. Simultaneously, in situ-forming hydrogel can perfectly fill cavities of any shapes after injection, thus adapting to requirements of various biological applications.[9,10] For example, Schiff based hydrogel prepared from oxidized alginate dialdehyde and gelatin was used to fill the site of meniscal tears for tissue repair.[11] Thermosensitive drug-loaded hydrogels were delivered by injection into the tumor (near and inside) and into the postoperative cavity for tumor therapy.[12-14] Poly(ethylene glycol) (PEG) based hydrogel with antibacterial performance was applied for promoting wound healing.[15]

Injectable hydrogels can be formed in situ either by chemical bonding or physical crosslinking such as chain entanglements,

* Corresponding authors.
E-mail addresses: sufeng@qust.edu.cn (F. Su), liufusheng63@sina.com (F. Liu), suming.li@umontpellier.fr (S. Li).

hydrophobic or ionic interactions, and hydrogen bonding.[16] The major advantage of physical hydrogels is that no crosslinking agent is required, but physical hydrogels generally have low stability. In contrast, chemical hydrogels can achieve a wider range of physicochemical properties while ensuring the biocompatibility.[17] Photo-crosslinking based on free radical polymerization has emerged as a promising strategy to prepare injectable chemical hydrogels due to mild reaction conditions, high reaction rate, low energy input and spatiotemporal control for hydrogel processing.[18,19] Acrylate functionalized natural and synthetic polymers such as gelatin, hyaluronic acid, chitosan, alginate, dextran and PEG have been extensively studied as photo-crosslinking materials for applications in tissue repair and regeneration, drug delivery, and cell culture.[20-23] In contrast to natural biopolymers, PEG is not degradable under *in vivo* conditions. In order to impart degradability to PEG based hydrogels, degradable copolymers have been prepared from PEG and degradable polyesters, including polylactide (PLA), poly(lactide-co-glycolide) (PLGA), poly(trimethylene carbonate) (PTMC) and poly(ε-caprolactone) (PCL).[24-27] One of the most relevant benefits is that hydrogels prepared from acrylate functionalized PEG-PLA, PEG-PLGA, PEG-PTMC and PEG-PCL copolymers are able to degrade in vivo into nontoxic molecules which can be metabolized or eliminated from the living organisms by renal excretion. Among the various degradable polymers, PCL has been widely investigated for uses as biomaterial due to its outstanding biodegradability and biocompatibility.[28-31]

Water soluble acrylated PCL-PEG-PCL (PEG-PCL-Acr) triblock copolymers have been used to prepare hydrogels as drug delivery vehicles and cell scaffolds.[32,33] Ko et al. synthesized photo-crosslinked PEG-PCL-Acr hydrogels to encapsulate chondrocytes and bone marrow stem cells for cartilage tissue engineering.[34] Data showed that the co-culture of both cell types in hydrogel provides an appropriate *in vitro* microenvironment for chondrogenic differentiation and cartilage matrix production. Xu et al. prepared PEG-PCL-Acr hydrogels for cell printing. Three types of human cells were bioprinted with the hydrogel to fabricate complex cell–gel constructs with high cell viability.[29] Multi-arm PEG-PCL block copolymers were also used to prepare photo-crosslinked hydrogels. Hou et al. studied the influence of arm number and copolymer concentration on the properties of hydrogels prepared from acrylated multi-arm copolymers.[35] The results showed that the gelation time, equilibrium swelling ratio, *in vitro* degradation, and drug release rate decreased with the increase of arm number and copolymer concentration. In our previous work, PEG-PTMC-Acr and 4 arm PEG-PCL-Acr hydrogels were prepared. The effects of copolymer concentration, hydrophilic/hydrophobic ratio, and block length on hydrogel properties and drug release behaviors were investigated.[36,37] Mixture of copolymers has also been tested to prepare hydrogels with specific properties. Xie et al. reported a cartilage-like hydrogel by mixing PEG-PCL-Acr and PEG-PLA-Acr for the repair of cartilage injury.[38]

In this work, a series of photo-crosslinked hydrogels were prepared by mixing PEG-PCL-Acr with acrylated PEG (PEG-Acr) or monomethoxy PEG (MPEG-Acr). The addition of mono-acrylated MPEG or diacrylated PEG is expected to tune the hydrogel properties and drug release behaviors. Photo-crosslinked hydrogels were prepared from mixture solutions of PEG-PCL-Acr and PEG-Acr or MPEG-Acr at different contents, using lithium phenyl-2,4,6-trimethylbenzoylphosphinate (LAP) as photo-initiator and visible light as light source. The internal morphology, swelling behavior, enzymatic degradation, and cyto-compatibility of hydrogels were investigated. Drug release behavior was evaluated *in vitro* using doxorubicin (DOX) as a model of hydrophilic anti-tumor drugs. The antitumor activity of drug-loaded hydrogels was evaluated *in vitro* using A549 cancer cell line. Most importantly, in situ gelation was achieved by subcutaneous injection of a hydrogel precursor solution containing polymers, LAP and DOX, followed by exposure to a light source, thus illustrating the feasibility of in situ preparation of drug delivery systems using minimally invasive method.

Methods

Materials

Monomethoxy PEG with Mn of 5000 g/mol ($MPEG_{5K}$), and PEG with Mn of 10000 g/mol (PEG_{10K}) were supplied by Sigma-Aldrich. PEG with Mn of 5000 g/mol (PEG_{5K}) was purchased from Bidepharm. Stannous octoate ($Sn(Oct)_2$), acryloyl chloride, triethylamine (TEA), ε–caprolactone (ε–CL), doxorubicin hydrochloride (DOX) and lipase from porcine pancreas (20 U/mg) were obtained from Aladdin. Dichloromethane and ε–CL were dried over calcium hydride (CaH_2) and distilled prior to use. Acryloyl chloride was dried over CaH_2. All other chemicals and solvents were used as received.

L929 cells were obtained from ATCC (USA). Dulbecco's modified eagle medium (DMEM), penicillin-streptomycin, fetal bovine serum, and 3-(4,5)-dimethylthiahiazo(-z-y1)-3,5-di-phenytetrazo-liumromide (MTT) were supplied by Thermo Fisher Scientific, Ltd. (China). Male Kunming mice, aged eight weeks, were supplied by Jinan Pengyue Experimental Animal Breeding Co., Ltd. (China). Animal care was made in accordance with the Guide for the Care and Use of Laboratory Animals, and the in vivo experiments were approved by the Ethics Committee for Animal Experimentation of Qingdao University of Science and Technology (Document No. 2017-1).

Synthesis and Characterization of Polymers

PEG-PCL-Acr was synthesized by using a two-step procedure.[37] Briefly, 10 g of PEG_{10K} (1.0 mmol), 2.28 g of ε–caprolactone (20.0 mmol) and 2.28 mg of $Sn(Oct)_2$ were added in a dried flask. The system was purged three times, and sealed under vacuum. Polymerization then proceeded at 130℃ for 72 h. The crude product was dissolved in dichloromethane, and the solution was precipitated by addition of diethyl ether. Finally, the product was vacuum dried to remove all organic solvents.

The resulted PCL-PEG_{10K}-PCL triblock copolymer was then functionalized by esterification with acryloyl chloride. TEA and acryloyl chloride were dropwise added to the copolymer solution in dichloromethane. The system was stirred for 1 h at 0 ℃, and then heated to 40 ℃. The reaction proceeded for 24 h under N_2 protection. The crude product was purified by precipitation in diethyl ether, dialysis against distilled water, and freeze drying. The obtained product was noted as PEG_{10K}-PCL-Acr. Acrylated $MPEG_{5K}$-Acr and PEG_{5K}-Acr were synthesized from $MPEG_{5K}$ or PEG_{5K} under similar conditions.

Preparation and Characterization of Photo-Crosslinked Hydrogels

Photo-crosslinked hydrogels were prepared from acrylated polymers by exposure to visible light using LAP as photoinitiator.[39,40] Typically, LAP (0.05 ‰ w/v) and polymers (10% w/v) were added to distilled water (1 mL). After complete dissolution, the reaction system was exposed to visible light (405 nm, 3 W) for 2 min, yielding a photo-crosslinked hydrogel at a concentration of 10%.

The feasibility of in situ gelation was assessed by subcutaneous injection of a hydrogel precursor solution in the abdomen of mice, followed by exposure to visible light. LAP (0.05 ‰ w/v), polymers (10% w/v) and DOX (0.05 % w/v) were dissolved to distilled water (1 mL). The solution was sterilized by filtration through a 0.22 μm membrane. Then, 200 μL solution was subcutaneously injected into the abdomen of mouse by using a sterile syringe equipped with a 22 G needle. The area of injection was exposed to visible light (405 nm, 3 W) for 2 min.

Characterization

Proton nuclear magnetic resonance (^{1}H NMR) spectra was registered using Avance-500 spectrometer (Bruker Daltonics Inc., Billerica, MA, USA) at 500 MHz. Chemical shifts (δ) were reported in ppm. Tetramethylsilane was used as internal reference, and deuterated chloroform ($CDCl_3$) as solvent.

Fourier transform infrared spectroscopy (FT-IR) spectra was recorded on TENSOR 27 FT-IR spectrometer (Bruker Optics, Germany). Samples were prepared using potassium bromide (KBr) pellet method. 32 scans were made for each measurement in the wavenumber range of 400 - 4000 cm^{-1}.

Scanning electron microscopy (SEM) was performed on JCM-7000 microscope (JEOL NeoScope, Japan). The accelerating voltage was 10.0 kV. Hydrogel samples were quenched in liquid nitrogen, lyophilized, and carefully fractured. Observation was then made after gold sputtering.

Swelling of Hydrogels

The gravimetric method was adopted to evaluate the degree of swelling and weight loss of hydrogels. As prepared hydrogels were placed in phosphate buffered saline (PBS) at pH 7.4 containing 0.1% sodium azide. After 72 h swelling at 25°C, the swollen samples were taken out and weighed. Finally, the samples were lyophilized and weighed again. The swelling ratio and gel content were calculated according to the following equations:

$$\textit{Swelling ratio}\ (\%) = \frac{W_s - W_d}{W_d} \times 100 \quad (1)$$

$$\textit{Gel content}\ (\%) = \frac{W_d}{W_0} \times 100 \quad (2)$$

Where W_0 is the weight of polymers used to prepare hydrogel samples, W_s is the weight of swollen hydrogels, and W_d is the remaining weight of lyophilized hydrogels.

Degradation of Hydrogel In vitro

In vitro degradation was achieved in the presence of lipase from porcine pancreas. As-prepared hydrogels were first swollen in deionized water for 72 h at 25°C so as to extract uncrosslinked water-soluble species from the network, and then freeze-dried. The obtained dried samples were immersed in 20 mL pH 7.4 PBS containing lipase at a concentration of 2 mg/mL. 0.1% sodium azide was added to the degradation medium as a bactericide. *In vitro* degradation was conducted at 37 ℃ under constant shaking (100 rpm). The medium was renewed with equal amount of fresh enzyme solution twice a week. At preset time intervals, the samples were withdrawn from the medium and freeze-dried. Three parallel experiments were made for each data point. The hydrogel weight loss was calculated from the following equation:

$$\textit{Weight loss}\ (\%) = \frac{W_i - W_t}{W_i} \times 100 \quad (3)$$

Where W_i and W_t refer to the initial dry weight and the remaining weight at time t, respectively.

Cyto-Toxicity Assay

The cyto-toxicity of the hydrogels was determined by MTT assay. Hydrogel extracts were prepared by soaking freeze-dried hydrogels in PBS at various concentrations from 0.5 to 5.0 mg/mL for 72 h. L929 and HUVEC cell suspensions were prepared in DMEM containing 10% FBS, 100 U/mL penicillin and 100 μg/mL streptomycin at a concentration of 2×10^5 cells/mL. In each well of a 96-well plate, 100 μL cell suspension was added. Cell culture proceeded for 24 h at 37℃ in an environment composed of 5% CO_2 and 95 % humidity to allow cell adhesion. Transwell inserts with a polycarbonate porous membrane (0.4 μm pore size), containing 100 μL hydrogel extract, were placed in wells. 100 μL hydrogel extract was then added. After 72 h, the culture medium was removed, and replaced by 100 μL fresh DMEM. 0.1 mg MTT was added, and cell culture continued for 4 h. Finally, all medium was removed, and 150 μL DMSO was added to fully dissolve crystallized formazan. The OD value of the DMSO solution was determined at 490 nm. DMEM was selected as the negative control, and a 0.5% aqueous solution of phenol as the positive control. The relative growth rate (RGR) was calculated according to the following equation:

$$\textit{RGR}\ (\%) = \frac{OD_{\textit{test sample}}}{OD_{\textit{negative control}}} \times 100 \quad (4)$$

In vitro *Drug Release*

Drug loaded hydrogels were prepared by in situ photo-crosslinking of drug containing precursor solutions.[41] Typically, LAP (0.5 mg), polymers (100 mg) and DOX (0.5 mg) were added in 1 mL distilled water. The solution was exposed to visible light (405 nm, 3 W) for 2 min, yielding a drug loaded hydrogel. In vitro drug release was performed at 37°C by soaking drug-loaded hydrogel in 5 mL PBS (pH 7.4). At predetermined time intervals, the total release solution was collected, and the same amount of fresh PBS was added. The absorbance of collected release solutions was measured at 490 nm. The accumulative amount of released drug was calculated on the basis of a previously established calibration curve of DOX.

In vitro *Anticancer Activity*

MTT assay was used to determine the anti-tumor effect of drug-loaded hydrogels as described above (Section 2.6), in comparison with free drug and blank hydrogels. Human lung cancer A549 cell line was selected to evaluate the proliferation inhibitory effect of drug-loaded hydrogels. Untreated cells were taken as a negative control group.

Statistical Analysis

All the experiments were performed in triplicates for 3 or 5 independent times. The data were revealed as mean ± standard deviation. Statistical analyses were carried out by the sample t-test, using OriginPro 2022 software package. Values with $p > 0.05$ were considered not significant, $^*p < 0.05$ statistically significant, $^{**}p < 0.01$ very significant, and $^{***}p < 0.001$ extremely significant.

Results and Discussion

Characterization of Polymers

A PCL-PEG_{10K}-PCL triblock copolymer was synthesized by ring opening polymerization (ROP) of ε−caprolactone in the presence of PEG_{10K} as macro-initiator and $Sn(Oct)_2$ as catalyst (Scheme 1). The ε−caprolactone/PEG molar ratio was 20. The resulted copolymer was end functionalized by reaction with acryloyl chloride to yield PEG_{10K}-PCL-Acr. Similarly, acrylated $MPEG_{5K}$-Acr and PEG_{5K}-Acr were synthesized from $MPEG_{5K}$ and PEG_{5K} using the same procedure, respectively (Scheme 1).

The chemical structure of the functionalized polymers was studied by ^{1}H NMR. As shown in Fig. 1, the signal **a** at 3.66 ppm belongs

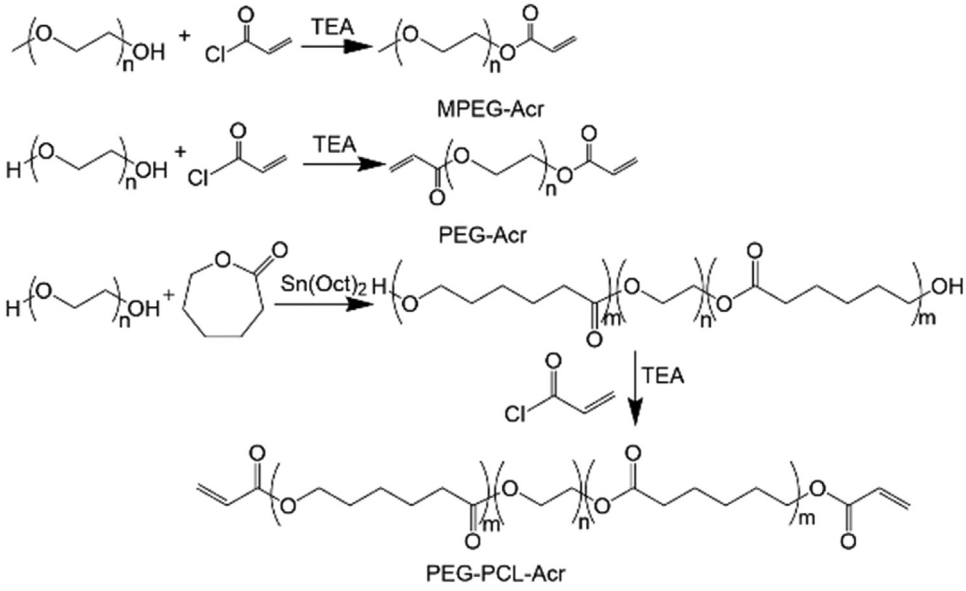

Scheme 1. Synthesis route of acrylate functionalized $MPEG_{5K}$-Acr, PEG_{5K}-Acr and PEG_{10K}-PCL-Acr polymers.

to the main chain methylene protons of PEG_{5K}-Acr or $MPEG_{5K}$-Acr. The signal **h** at 3.35 ppm belongs to the terminal methyl group of $MPEG_{5K}$-Acr. The signals **b, c, d, e** at 1.38, 1.65, 2.31 and 4.07 ppm are attributed to the different methylene groups of PCL block in the triblock copolymer. The signals **f** and **g** detected in 5.60-6.30 ppm are assigned to the acryloyl group of functionalized chain ends.

The degree of polymerization (DP) of PCL blocks in the triblock copolymer was determined from the integrations of signals **c** and **a**. A value of 18 was obtained, which is close to the feed ratio. The total Mn of PCL blocks was 2000 as determined from the DP of PCL blocks and the molar mass of caprolactone. The triblock copolymer is thus noted as PCL_{1k}-PEG_{10K}-PCL_{1k}, and the functionalized one as PEG_{10K}-PCL_{2k}-Acr. The degree of substitution (DS) of chain ends by the acryloyl group was calculated from the integration of signals **f** and **a**. The DS of $MPEG_{5K}$-Acr, PEG_{5K}-Acr, and PEG_{10K}-PCL_{2k}-Acr was 59.1%, 60.2% and 75.2%, indicating successful acrylation of the hydroxyl end groups. It is noteworthy that the DS of PCL-PEG-PCL copolymer is higher than that of PEG and MPEG. Similar findings have been reported in the case of PTMC-PEG-PTMC and 4-arm PEG-PCL copolymers.[36,37]

FT-IR spectroscopy was also used to investigate the chemical structures of polymers. Fig. 2 shows the FT-IR spectra of the polymers before and after functionalization. Both PEG_{5K} and $MPEG_{5K}$ present two main bands at 2880 and 1110 cm^{-1} which are assigned to the stretching vibration of CH_2 and C-O-C (Fig. 2D, 2F), respectively. The triblock copolymer PCL_{10k}-PEG_{10K}-PCL_{1k} presents a band at 1730 cm^{-1} due to the stretching vibration of carbonyl group, and a band at 2880 cm^{-1} assigned to the stretching vibration of CH_2 groups (Fig. 2B). On the spectra of PEG_{10K}-PCL_{2k}-Acr (Fig. 2A), PEG_{5K}-Acr (Fig. 2C), and $MPEG_{5K}$-Acr (Fig. 2E), the characteristic band of the C=C double bond is detected at 1640 cm^{-1}, indicating their successful functionalization. Moreover, PEG_{5K}-Acr and $MPEG_{5K}$-Acr exhibit a

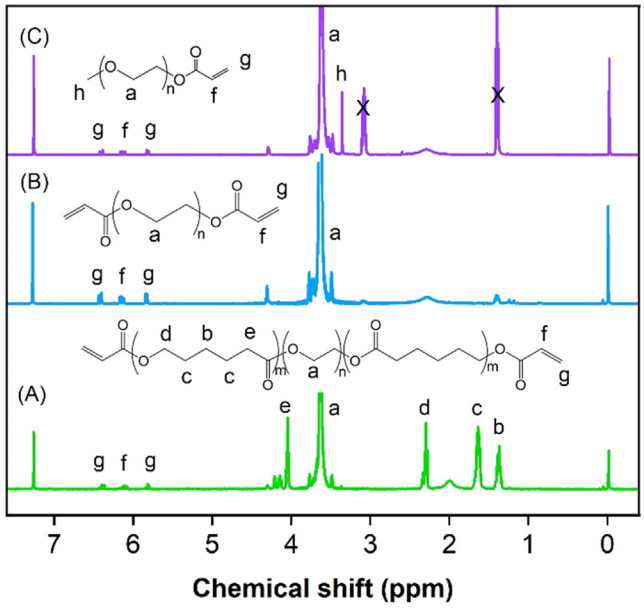

Figure 1. ^1H NMR spectra of PEG_{10K}-PCL_{2k}-Acr (A), PEG_{5K}-Acr, (B) and $MPEG_{5K}$-Acr (C) in $CDCl_3$.

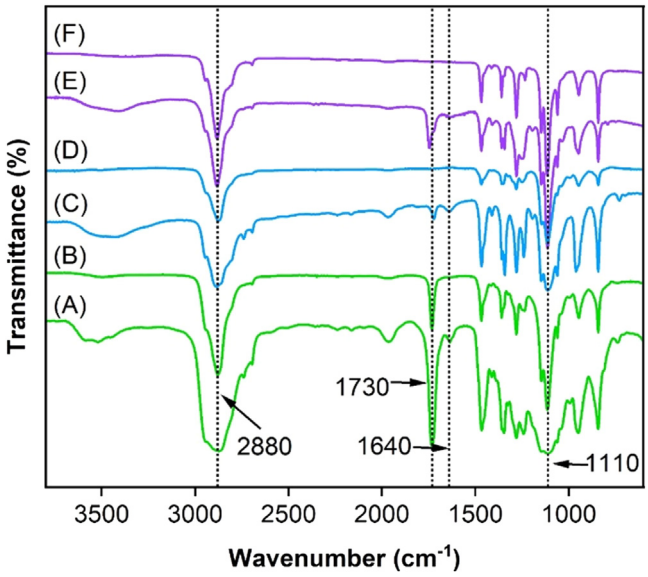

Figure 2. FT-IR spectra of PEG_{10K}-PCL_{2k}-Acr (A), PCL_{1k}-PEG_{10K}-PCL_{1k} (B), PEG_{5K}-Acr, (C), PEG_{5K} (D), $MPEG_{5K}$-Acr (E), and $MPEG_{5K}$ (F).

small band at 1730 cm^{-1}, which further confirms the functionalization with attachment of acrylate group.

Characterization of Hydrogels

A series of hydrogels were prepared by crosslinking of acrylated polymers via free radical polymerization. LAP, synthesized as previously reported,[36,37] was selected as photoinitiator to generate free radicals under visible light irradiation. Blank and DOX-loaded photocrosslinked hydrogels were successfully prepared *in vitro* from precursor solutions by exposure to visible light at 405 nm for 2 min as LAP has maximum absorption at 365 and 405 nm. The whole preparation process is simple, safe and fast. Importantly, the use of visible light sources ensures the safety of the procedure for biological applications. Gelation using visible light is not concern when preparing the injection. In fact, the wavelength range of visible light is very large. Thus the light intensity at a specific wavelength is not sufficient to initiate photopolymerization during the preparation of solutions.

The composition of the various copolymers is shown in Table 1. Mixtures of PEG_{10K}-PCL_{2K}-Acr and $MPEG_{5K}$-Acr or PEG_{5K}-Acr were used in order to modulate the properties of resulted hydrogels. Hydrogels obtained from mixtures of PEG_{10K}-PCL_{2K}-Acr and $MPEG_{5K}$-Acr are named as MPAx, and those obtained from mixtures of PEG_{10K}-PCL_{2K}-Acr and PEG_{5K}-Acr are named as PAx, with x designating the content (%) of $MPEG_{5K}$-Acr or PEG_{5K}-Acr in the hydrogels. On the other hand, hydrogel prepared from pure PEG_{10K}-PCL_{2K}-Acr is abbreviated as PPA.

In situ gelation was realized by subcutaneous injection of 200 μL of sterilized hydrogel precursor solution into the abdomen of mice. The injected area was immediately irradiated with 405 nm wavelength visible light for 2 min. Abdominal skin tissue was then carefully peeled off. A well formed hydrogel was obtained (Fig. 3). DOX-loaded hydrogel was also obtained under similar conditions, thus illustrating the in-situ gelation of drug-loaded precursor solutions. In other words, in-situ construction of a local drug delivery system is feasible. Elisseeff et al. previously explored the efficiency of UVA and visible light transmission through pig skin to initiate photo-polymerization of poly(ethylene oxide) dimethacrylate.[42] Methacrylated chitosan and gelatin solutions have also been subjected to transdermal gelation by UV light irradiation for applications in tissue engineering and drug delivery.[43,44] In this work, visible light-initiated polymerization is applied to provide a safer strategy for in situ gelation *in vivo*, which is of major importance for the clinical applications of topical drug delivery systems.

Hydrogels are able to swell in an aqueous medium by absorbing large amounts of water without dissolving. It is known that the swelling properties of photo-crosslinked hydrogels prepared from amphiphilic copolymers are dependent on the polymer concentration and hydrophilic/hydrophobic balance.[29,35,37] Hydrogels with desired properties can also be obtained by mixing two copolymers in the precursor solution.[38] Nevertheless, weight loss is often observed during swelling as uncrosslinked components can diffuse out and be dissolved in the medium.

The swelling and weight loss ratios of the hydrogels were determined by soaking as prepared hydrogels in deionized water for 72 h at 25°C to reach the swelling equilibrium. The medium was regularly changed so as to facilitate removal of uncrosslinked polymers. As shown in Fig. 4A, the swelling ratio of PPA hydrogel is 1704%, and the gel content is 85%. MPA10, MPA20 and MPA50 hydrogels present a swelling ratio of 2103, 3093, and 4735%, and a gel content of 76, 68 and 64%, respectively. Thus the ability of MPA hydrogels to absorb water is significantly improved as compared to PPA hydrogel due to the addition of MPEG-Acr component. In fact, PEG-PCL-Acr is acrylated at both chain ends, and is thus fully involved in the photo-crosslinked network. In contrast, MPEG-Acr is acrylated at one chain end only, and is attached to the network as pendant chains. As a consequence, MPA hydrogels exhibit a looser network structure with lower crosslink density as compared to PPA hydrogel. Higher MPEG-Acr content leads to lower crosslinking density, resulting in higher swelling and lower gel content. It is also noteworthy that higher MPEG-Acr content increases the hydrophilic/hydrophobic balance in MPA hydrogels, which favors water absorption. On the other hand, lower gel content also favors water absorption as more space is available for water absorption.

The swelling ratio of PA10, PA20, PA50 and PA80 hydrogels is 1922, 2029, 2629 and 3158%, respectively, suggesting an increasing trend of swelling ratio with increasing PEG-Acr content. Meanwhile, the gel content of PA hydrogels decreases from 81% for PA10 to 75% for PA80. Higher PEG-Acr content and lower gel content both favor water absorption. It is also noted that PA hydrogels present higher swelling ratio and lower gel content than PPA hydrogel because of the lower PEG content of the latter. In contrast, PA hydrogels present lower swelling ratio and higher gel content than MPA hydrogels with the same PEG contents, which could be attributed to the looser network structure and lower crosslink density of MPA hydrogels. These findings demonstrate the possibility to tailor in a large range the swelling behavior of hydrogels prepared from acrylated amphiphilic copolymers by addition of PEG-Acr and/or MPEG-Acr of various contents.

Photo-crosslinked hydrogels contain hydrolyzable bonds in the network, including both acrylate groups and PCL ester bonds, which provides the network with degradability.[45] PCL degrades very slowly by pure hydrolysis,[46] but its degradation is strongly accelerated in the presence of lipases.[47] The degradation behavior of hydrogels was determined by using lipase from porcine pancreas as lipases could be involved in the in vivo degradation of PCL based materials.[47] As prepared hydrogels were first subjected to swelling-lyophilization treatment so as to eliminate uncrosslinked species. As shown in Fig. 4B, almost linear increase of weight loss is observed in all cases during the whole degradation period up to 4 weeks. MPA20 hydrogel presents the fastest degradation rate, reaching a weight loss of 27.9% after 4 weeks. This is followed by MPA10 hydrogel (22.7%) and PPA hydrogel (21.7%). The higher degradation rate of MPA as compared to PPA can be explained by the crosslinked structure of both hydrogels prepared from MPEG-Acr and/or PEG-PCL-Acr. The attachment of MPEG-Acr with a single reaction site in the network leads to looser network structure, resulting in high swelling ratio that facilitates entry of enzyme and water molecules. Once the acrylate linkage between PCL and MPEG is broken, MPEG block will be detached from the hydrogel. In contrast, the detachment of PEG block is less easier as it is included in the network at both sides. On the other hand, the degradation rates of PA hydrogels are all lower than those of PPA and MPA hydrogels, and the final weight loss values vary from 11.8 to 20.4%. In fact, the addition of diacrylated PEG component in PA

Table 1
Compositions of Hydrogels Prepared from Acrylated PEG_{10K}-PCL_{2K}-Acr, PEG_{5K}-Acr and $MPEG_{5K}$-Acr.

Hydrogel	MPA10	MPA20	MPA50	PA10	PA20	PA50	PA80	PPA
PEG_{10K}-PCL_{2K}-Acr (%)	90	80	50	90	80	50	20	100
PEG_{5K}-Acr (%)	0	0	0	10	20	50	80	0
$MPEG_{5K}$-Acr (%)	10	20	50	0	0	0	0	0

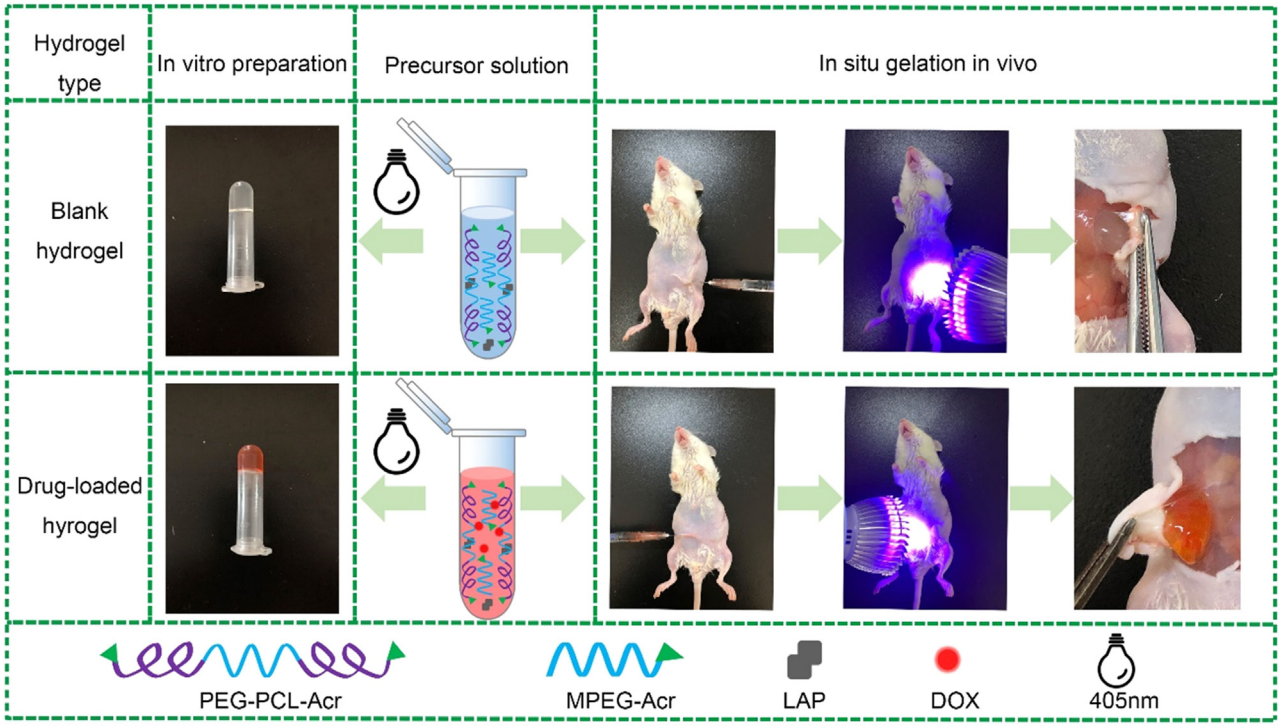

Figure 3. *In vivo* and *in vitro* preparation of blank and drug-loaded hydrogels by visible light irradiation of acrylated polymers in the presence of LAP.

hydrogels results in higher crosslink density and lower PCL content as compared to PPA and MPA hydrogels. Thus there are less ester bonds available for enzymatic hydrolysis, leading to slower degradation. The higher the PEG-Acr content, the slower the degradation. Therefore, the degradation rate of hydrogels prepared from acrylated PEG-PCL, PEG and MPEG can be tailored by varying the material composition. Degradation mainly results from enzymatic cleavage of PCL ester bonds, as well as acrylate end groups.[46-49]

The water absorption and drug release behavior of hydrogels are closely related to the network structure. The internal morphology of as prepared MPA20, PA20 and PPA hydrogels was observed by using SEM as shown in Fig. 5. All hydrogels exhibit a uniformly distributed and interconnected porous structure. Similar structures are observed for other hydrogels (Fig. S1).

Cyto-Toxicity Assay

Based on the enzymatic reduction of MTT by living cells, the formation of formazan crystals is proportional to cell viability. MTT assay is thus widely applied to evaluate the cytocompatibility of biomaterials. In this work, L929 cells from mice and human HUVEC cells were used to determine the cyto-toxicity of hydrogels. As shown in Fig. 6A, the RGR of DMEM selected as negative control is 100%, and that of 0.5% phenol solution selected as positive controls is 20%. After co-culture with MPA, PA and PPA hydrogels for 72 h, the RGR values of L929 cells are all above 90% in the concentration range from 0.5 to 5.0 mg/mL (Fig. 6A). Similar results are obtained for HUVEC cells (Fig. 6B). According to the US Pharmacopeia Standards and ISO 10993, the hydrogels present excellent cytocompatibility.

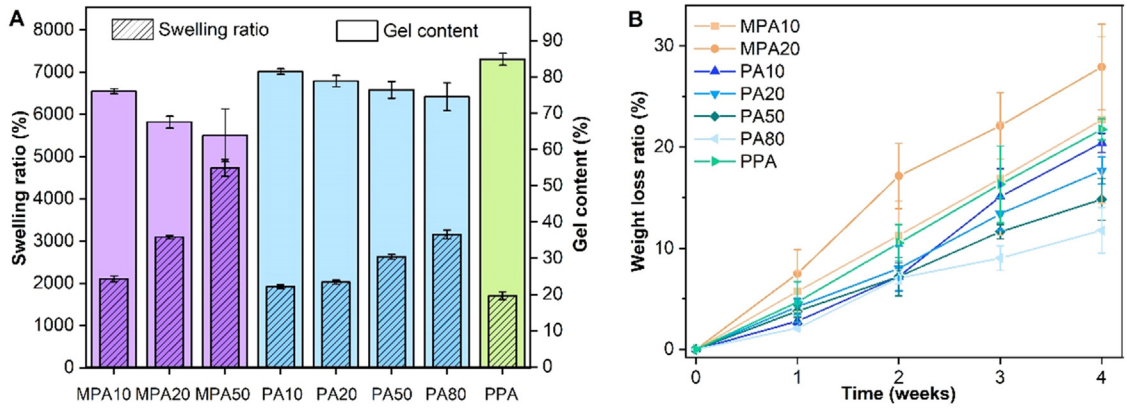

Figure 4. Swelling ratio and gel content data of hydrogels (A), variation of weight loss ratio of hydrogels during degradation in the presence of lipase (B).

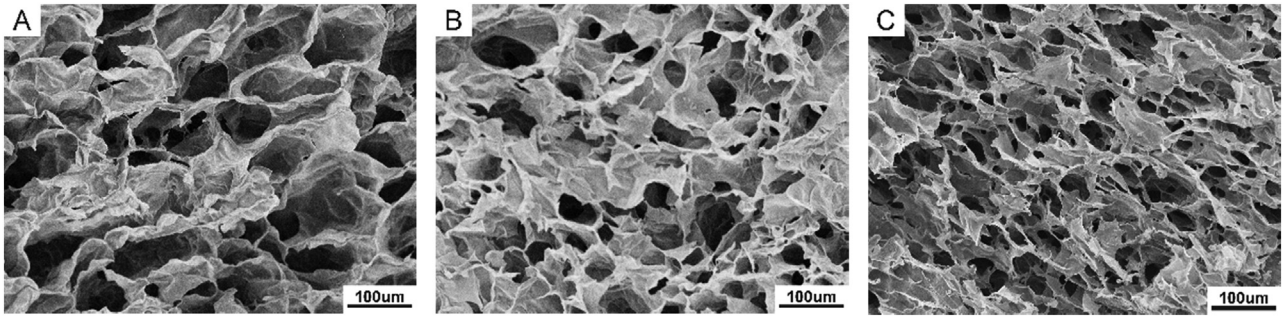

Figure 5. SEM images of as prepared MPA20 (A), PA20 (B), and PPA (C) hydrogels.

In vitro *Drug Release*

DOX is one of the most efficient chemotherapeutic drugs, but it has important adverse effects on myocardial cells, limiting its clinical applications. Local drug delivery systems can avoid the first-pass effect and locally release the drug, especially for the treatment of solid tumors. Thus DOX-containing hydrogel precursor solution can be administered to the lesion site through a syringe, which can maximize the effective drug delivery and minimize the toxic side effects.

Drug loading was realized during in-situ gelation. It is thus considered that initially added drug was totally encapsulated. Photocrosslinked drug-loaded hydrogels were immersed in 5 mL PBS to assess drug release behaviors. As illustrated in Fig. 7A, PPA hydrogel has the slowest release profile. The drug release ratio of MPA10, MPA20, MPA50 and PPA is 9.3, 15.6, 31.2 and 7.2% after 24 h, respectively, and reaches 52.8, 58.9, 77.6 and 48.6% after 28 days. Thus with increase of MPEG content, the drug release rate shows an increasing trend. This finding can be assigned to the reduced crosslinking density with increasing MPEG content since loose network facilitates drug diffusion, in agreement with swelling data.

Similar drug release trends are observed for PA hydrogels as shown in Fig. 7B. The drug release rate of PA10, PA20, PA50 and PA80 is 12.1%, 14.2%, 17.2% and 23.3% after 24 h, respectively, and increases to 49.7%, 54.9%, 66.1% and 87.5% after 28 days. The higher the PEG content, the higher the release rate because drug release is enhanced by swelling. Similarly, the drug release rate from PA hydrogels is higher than that from PPA hydrogel. It has been shown that purely hydrophilic hydrogels exhibit very fast drug release, while the addition of hydrophobic blocks decreases the release rate.[6] It is worth mentioning that, for the same PEG or MPEG content, the drug release from MPA20 or MPA 50 is faster than that from PA20 or PA50.

In our previous work, PEG-PTMC-Acr and 4aPEG-PCL-Acr photocrosslinked hydrogels were prepared, and drug loading was achieved by soaking freeze dried gels in drug solutions. Biphasic drug release profiles were obtained with strong burst release up to 50% after 24 h.[36,37] The strategy of in situ drug loading allows to greatly reduce burst drug release (7.2% drug release from PPA hydrogel at 24 h), and to maintain a sustained drug release at a later stage.

In vitro *Anticancer Activity*

The cyto-toxicity of blank hydrogels against A549 lung cancer cells was first tested. As shown in Fig. 8A, the RGR values of all the hydrogels are well above 90% after 72 h co-culture, showing that blank hydrogels have no effect on A549 cells.

As a cycle non-specific antitumor drug, DOX is able to inhibit the synthesis of RNA and DNA, and kill tumor cells of various growth cycles. A549 lung cancer cells were selected to evaluate the antitumor activity of 5 selected drug loaded hydrogels, MPA20, MPA50, PA20, PA50, and PPA, in comparison free drug (Fig. 8B). The amount of free drug was equal to the drug content of DOX-loaded hydrogels. As shown in Fig. 8B, the RGR decreases or the antitumor activity increases with increasing drug concentration from 12.5 to 50.0 μg/mL. The antitumor activity of PPA hydrogel is lower than that of MPA and PA mixture hydrogels. On the other hand, MPA hydrogels exhibit slightly higher activity than corresponding PA hydrogels at concentrations of 12.5 and 25 μg/mL, and mixture hydrogels containing 50% PEG or MPEG exhibit slightly higher activity than those containing 20% PEG or MPEG. These differences are closely related to drug release behavior of the various systems. Faster drug release leads to higher tumor proliferation inhibitive effect, especially in the first days. It is also noteworthy that free drug exhibits slightly higher

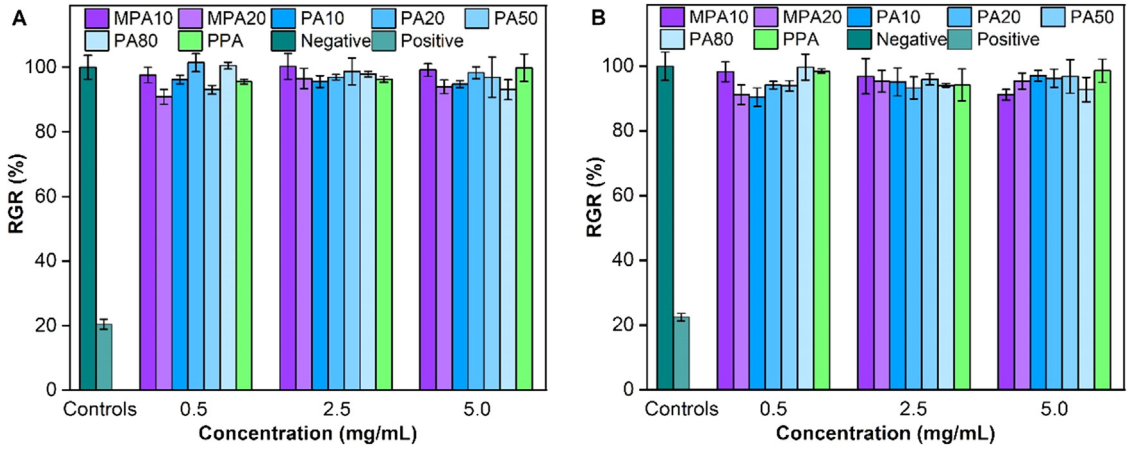

Figure 6. RGR data of L929 cells and HUVEC cells after 72 h culture with hydrogels at different concentrations.

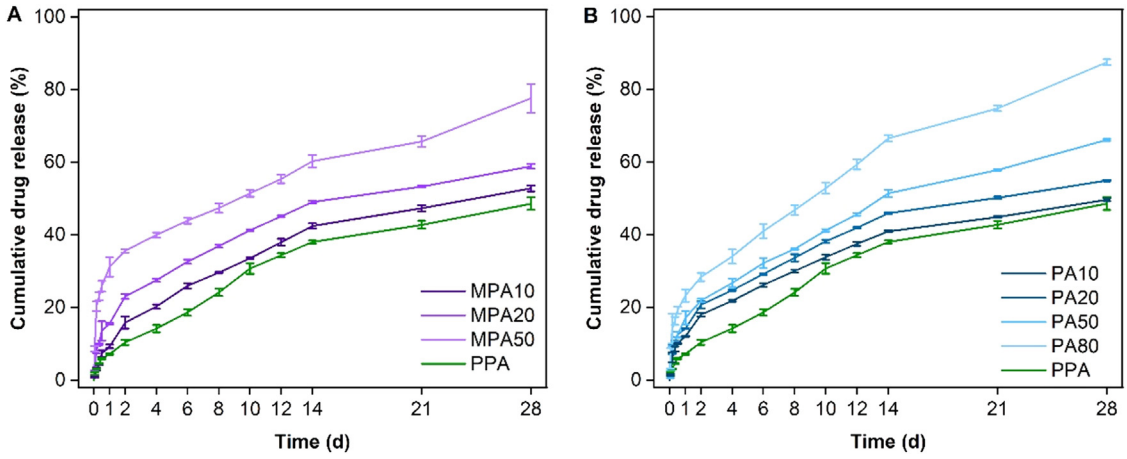

Figure 7. A) Cumulative drug release from DOX-loaded MPA20, MPA50, and PPA hydrogels, (B) cumulative drug release from DOX-loaded PA20, PA50, and PPA hydrogels.

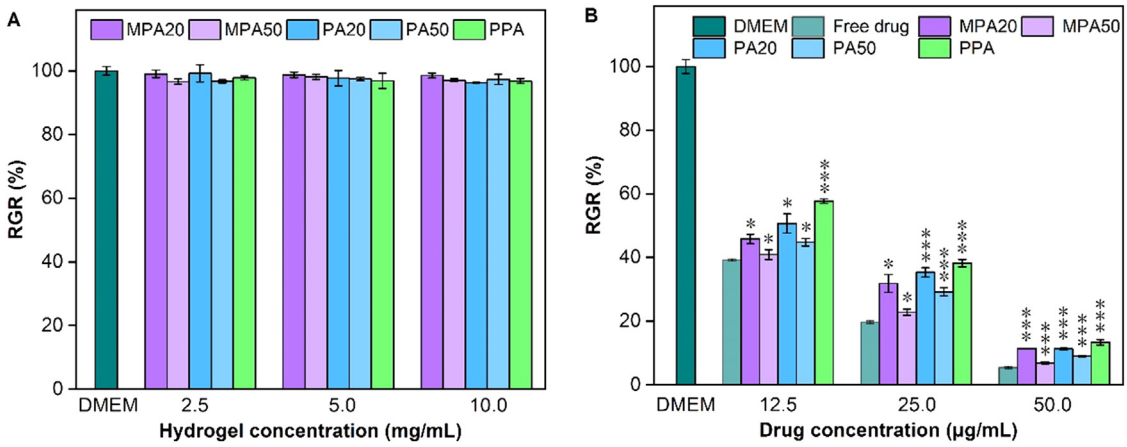

Figure 8. A) RGR data of A549 cells after 72 h co-culture MPA20, MPA50, PA20, PA50, and PPA hydrogels, (B) RGR data of A549 cells after 72 h co-culture with free drug and DOX-loaded MPA20, MPA50, PA20, PA50, and PPA hydrogels at concentration of 12.5, 25, and 50.0 μg/mL.

antitumor activity than drug loaded hydrogels. Nevertheless, taking into account the sustained-release behavior and biodegradability, drug loaded hydrogels could be very promising for long-term treatment.

Conclusion

A series of photo-crosslinked PEG-PCL-Acr hydrogels containing MPEG-Acr and or PEG-Acr were prepared by using visible light as light source and LAP as initiator. The properties of hydrogels can be tuned by adding MPEG-Acr or PEG-Acr with different contents. The addition of MPEG-Acr with single reactive site reduces the cross-linking density, resulting in higher swelling ratio as compared to PEG-PCL-Acr hydrogel. Addition of diacrylated PEG-Acr also leads to increase of the swelling ratio due to higher hydrophilic content. MPA hydrogels with loose network degrades faster than PPA and PA hydrogels in the presence of lipase as MPEG blocks can be more easily detached from the network as compared to PEG blocks. In contrast, the degradation of PA is slower than that of PPA due to less degradable sites.

All the hydrogels present outstanding cytocompatibility as shown by MTT assay using A929 and HUVEC cells. DOX-loaded hydrogel is obtained in situ by injection of a precursor solution in the abdomen of mice followed by exposure to visible light. Prolonged drug release up to 28 days is achieved under in vitro conditions, the release rate depending on the network structure and hydrophilic content of hydrogels. Last but not least, DOX-loaded hydrogels present outstanding proliferation inhibitive effect against cancer cells in comparison with free drug. Therefore, mixture hydrogels prepared from acrylated PEG-PCL and PEG or MPEG with tunable properties could be most promising for the construction of local drug delivery systems in cancer therapy.

Declaration of Competing Interest

The authors declare that they have no known competing financial interests or personal relationships that could have appeared to influence the work reported in this paper.

Acknowledgments

The work was financially supported by the Shandong Provincial Natural Science Foundation (ZR2021ME208, ZR2022ME083) and Postdoctoral Applied Research Project of Qingdao Municipality.

Supplementary Materials

Supplementary material associated with this article can be found in the online version at doi:10.1016/j.xphs.2023.02.004.

References

1. Wichterle O, LÍM D. Hydrophilic gels for biological use. *Nature*. 1960;185:117–118. https://doi.org/10.1038/185117a0.
2. Marques AC, Costa PJ, Velho S, Amaral MH. Stimuli-responsive hydrogels for intratumoral drug delivery. *Drug Discov Today*. 2021;26(10):2397–2405. https://doi.org/10.1016/j.drudis.2021.04.012.
3. Wang C, Wang M, Xu TZ, et al. Engineering bioactive self-healing antibacterial exosomes hydrogel for promoting chronic diabetic wound healing and complete skin regeneration. *Theranostics*. 2019;9(1):65–76. https://doi.org/10.7150/thno.29766.
4. Sivaraj D, Chen KL, Chattopadhyay A, et al. Hydrogel scaffolds to deliver cell therapies for wound healing. *Front Bioeng Biotech*. 2021;9: 660145. https://doi.org/10.3389/fbioe.2021.660145.
5. Brumberg V, Astrelina T, Malivanova T, Samoilova A. Modern wound dressings: hydrogel dressings. *Biomedicines*. 2021;9(9):1235. https://doi.org/10.3390/biomedicines9091235.
6. Li Y, Yang HY, Lee DS. Advances in biodegradable and injectable hydrogels for biomedical applications. *J Control Release*. 2021;330:151–160. https://doi.org/10.1016/j.jconrel.2020.12.008.
7. Rizzo F, Kehr NS. Recent advances in injectable hydrogels for controlled and local drug delivery. *Adv Healthc Mater*. 2021;10(1): 2001341. https://doi.org/10.1002/adhm.202001341.
8. Cirillo G, Spizzirri UG, Curcio M, Nicoletta FP, Lemma F. Injectable hydrogels for cancer therapy over the last decade. *Pharmaceutics*. 2019;11(9):486. https://doi.org/10.3390/pharmaceutics11090486.
9. Mohammadi M, Karimi M, Malaekeh-Nikouei B, Torkashvand M, Alibolandi M. Hybrid in situ-forming injectable hydrogels for local cancer therapy. *Int J Pharmaceut*. 2022;616: 121534. https://doi.org/10.1016/j.ijpharm.2022.121534.
10. Babu S, Albertino F, Anarkoli AO, De Laporte L. Controlling structure with injectable biomaterials to better mimic tissue heterogeneity and anisotropy. *Adv Healthc Mater*. 2021;10(11): 2002221. https://doi.org/10.1002/adhm.202002221.
11. Resmi R, Parvathy J, John A, Joseph R. Injectable self-crosslinking hydrogels for meniscal repair: a study with oxidized alginate and gelatin. *Carbohyd Polym*. 2020;234: 115902. https://doi.org/10.1016/j.carbpol.2020.115902.
12. Fu H, Huang LL, Xu CQ, et al. Highly biocompatible thermosensitive nanocomposite gel for combined therapy of hepatocellular carcinoma via the enhancement of mitochondria related apoptosis. *Nanomed-Nanotechnol*. 2019;21: 102062. https://doi.org/10.1016/j.nano.2019.102062.
13. He Y, Yuan TW, Wang X, et al. Temperature sensitive hydrogel for preoperative treatment of renal carcinoma. *Mater Sci Eng C*. 2020;111: 110798. https://doi.org/10.1016/j.msec.2020.110798.
14. Ding L, Wang Q, Shen M, et al. Thermoresponsive nanocomposite gel for local drug delivery to suppress the growth of glioma by inducing autophagy. *Autophagy*. 2017;13(7):1176–1190. https://doi.org/10.1080/15548627.2017.1320634.
15. Liu SJ, Jiang T, Guo RQ, et al. Injectable and degradable PEG hydrogel with antibacterial performance for promoting wound healing. *ACS Appl Bio Mater*. 2021;4 (3):2769–2780. https://doi.org/10.1021/acsabm.1c00004.
16. Alonso JM, del Olma JA, Gonzalez RP, Saez-Martinez V. Injectable hydrogels: from laboratory to industrialization. *Ploymers*. 2021;13(4):650. https://doi.org/10.3390/polym13040650.
17. Nezhad-Mokhtari P, Ghorbani M, Roshangar L, Rad JS. A review on the construction of hydrogel scaffolds by various chemically techniques for tissue engineering. *Eur Polym J*. 2019;117:64–76. https://doi.org/10.1016/j.eurpolymj.2019.05.004.
18. Zhu HY, Yang HQ, Ma YF, et al. Spatiotemporally controlled photoresponsive hydrogels: design and predictive modeling from processing through application. *Adv Funct Mater*. 2020;30(32): 2000639. https://doi.org/10.1002/adfm.202000639.
19. Choi JR, Yong KW, Choi JY, Cowie AC. Recent advances in photo-crosslinkable hydrogels for biomedical applications. *Biotechniques*. 2019;66(1):40–53. https://doi.org/10.2144/btn-2018-0083.
20. Nezhad-Mokhtari P, Ghorbani M, Roshangar L, Rad JS. Chemical gelling of hydrogels-based biological macromolecules for tissue engineering: photo- and enzymatic-crosslinking methods. *Int J Biol Macromol*. 2019;139:760–772. https://doi.org/10.1016/j.ijbiomac.2019.08.047.
21. Yang DH, Chun HJ. Visible light-curable hydrogel systems for tissue engineering and drug delivery. *Bioinspired Biomaterials: Advances in Tissue Engineering and Regenerative Medicine*. 1249. Springer; 2020:85–93. https://doi.org/10.1007/978-981-15-3258-0_6.
22. Samadian H, Maleki H, Allahyari Z, Jaymand M. Natural polymers-based light-induced hydrogels: promising biomaterials for biomedical applications. *Corrd Chem Rev*. 2020;420: 213432. https://doi.org/10.1016/j.ccr.2020.213432.
23. Zennifer A, Manivannan S, Sethuraman S, Kumbar SG, Sundaramurthi D. 3D bioprinting and photocrosslinking: emerging strategies and future perspectives. *Biomater Adv*. 2022;134: 112576. https://doi.org/10.1016/j.msec.2021.112576.
24. Shi JY, Yu L, Ding JD. PEG-based thermosensitive and biodegradable hydrogels. *Acta Biomater*. 2021;128:42–59. https://doi.org/10.1016/j.actbio.2021.04.009.
25. Munim SA, Raza ZA. Poly(lactic acid) based hydrogels: formation, characteristics and biomedical applications. *J Porous Mat*. 2019;26(3):881–901. https://doi.org/10.1007/s10934-018-0687-z.
26. Sharifi S, Blanquer SBG, van Kooten TG, Grijpma DW. Biodegradable nanocomposite hydrogel structures with enhanced mechanical properties prepared by photocrosslinking solutions of poly(trimethylene carbonate)−poly(ethylene glycol)−poly(trimethylene carbonate) macromonomers and nanoclay particles. *Acta Biomater*. 2012;8(12):4233–4243. https://doi.org/10.1016/j.actbio.2012.09.014.
27. Dethe MR, Prabakaran A, Ahmed H, Argrawal M, Roy U, Alexander A. PCL-PEG copolymer based injectable thermosensitive hydrogels. *J Control Release*. 2022: (343):217–236. https://doi.org/10.1016/j.jconrel.2022.01.035.
28. Dabbaghi A, Ramazani A, Farshchi N, Rezaei A, Bodaghi A, Rezayati S. Synthesis, physical and mechanical properties of amphiphilic hydrogels based on polycaprolactone and polyethylene glycol for bioapplications: a review. *J Ind Eng Chem*. 2021:(101):307–323. https://doi.org/10.1016/j.jiec.2021.05.051.
29. Xu CC, Lee WH, Dai GH, Hong Y. Highly elastic biodegradable single-network hydrogel for cell printing. *ACS Appl Mater Inter*. 2018;10(12):9969–9979. https://doi.org/10.1021/acsami.8b01294.
30. Lin GY, Cosimbescu L, Karin NJ, Gutowska A, Tarasevich BJ. Injectable and thermogelling hydrogels of PCL-g-PEG:mechanisms, rheological and enzymatic degradation properties. *J Mater Chem B*. 2013;1(9):1249–1255. https://doi.org/10.1039/c2tb00468b.
31. Boffito M, Sirianni P, Di Rienzo AM, Chiono V. Thermosensitive block copolymer hydrogels based on poly(ε-caprolactone) and polyethylene glycol for biomedical applications: State of the art and future perspectives. *J Biomed Mater Res A*. 2015;103(3):1276–1290. https://doi.org/10.1002/jbm.a.35253.
32. Khoee S, Kardani M. Preparation of PCL/PEG superporous hydrogel containing drug-loaded nanoparticles: the effect of hydrophobic−hydrophilic interface on the physical properties. *Eur Polym J*. 2014;58:180–190. https://doi.org/10.1016/j.eurpolymj.2014.06.024.
33. Soto-Quintero A, Meneses-Acosta A, Romo-Uribe A. Tailoring the viscoelastic, swelling kinetics and antibacterial behavior of poly(ethylene glycol)-based hydrogels with polycaprolactone. *Eur Polym J*. 2015;70:1–17. https://doi.org/10.1016/j.eurpolymj.2015.06.028.
34. Ko CY, Ku KL, Yang SR, et al. *In vitro* and *in vivo* co-culture of chondrocytes and bone marrow stem cells in photocrosslinked PCL−PEG−PCL hydrogels enhances cartilage formation. *J Tissue Eng Regen M*. 2016;10(10):483–496. https://doi.org/10.1002/term.1846.
35. Hou P, Zhang N, Wu RX, Xu WW, Hou ZS. Photo-cross-linked biodegradable hydrogels based on n-arm-poly(ethyleneglycol), poly(ε-caprolactone) and/or methacrylic acid for controlled drug release. *J Biomater Appl*. 2017;32(4):511–523. https://doi.org/10.1177/0885328217730465.
36. Wang YD, Xi LS, Zhang BG, et al. Bioresorbable hydrogels prepared by photo-initiated crosslinking of diacrylated PTMC-PEG-PTMC triblock copolymers as potential carrier of antitumor drugs. *Saudi Pharm J*. 2020;28(3):290–299. https://doi.org/10.1016/j.jsps.2020.01.008.
37. Wang YD, Wang SX, Hu WJ, Su F, Liu FS, Li SM. In situ photo-crosslinked hydrogels prepared from acrylated 4-arm-poly(ethylene glycol)-poly(ε-caprolactone) block copolymers for local cancer therapy. *Polym Advan Technol*. 2022;33(8):2620–2631. https://doi.org/10.1002/pat.5718.
38. Xie MS, Fritch M, He YC, Fu HK, Hong Y, Lin H. Dynamic loading enhances chondrogenesis of human chondrocytes within a biodegradable resilient hydrogel. *Biomater Sci*. 2021;9(14):5011–5024. https://doi.org/10.1039/d1bm00413a.
39. Majima T, Schnabel W, Weber W. Phenyl-2,4,6-trimethylbenzoylphosphinates as water-soluble photoinitiators. Generation and reactivity of $O{=}\dot{P}(C_6H_5)(O^-)$ radical anions. *Makromol Chem*. 1991;192(10):2307–2315. https://doi.org/10.1002/macp.1991.021921010.
40. Fairbanks BD, Schwartz MP, Bowman CN, Anseth KS. Photoinitiated polymerization of PEG-diacrylate with lithium phenyl-2,4,6-trimethylbenzoylphosphinate: Polymerization rate and cytocompatibility. *Biomaterials*. 2009;30(35):6702–6707. https://doi.org/10.1016/j.biomaterials.2009.08.055.
41. Huang SH, Liu HL, Huang SS, Fu TL, Xue W, Guo R. Dextran methacrylate hydrogel microneedles loaded with doxorubicin and trametinib for continuous transdermal administration of melanoma. *Carbohyd Polym*. 2020;246: 116650. https://doi.org/10.1016/j.carbpol.2020.116650.
42. Elisseeff J, Anseth K, Sims D, McIntosh W, Randolph M, Langer R. Transdermal photopolymerization for minimally invasive implantation. *Proc Natl Acad Sci USA*. 1999;96(6):3104–3107. https://doi.org/10.1073/pnas.96.6.3104.
43. Lin RZ, Chen YC, Melero-Martin JM. Transdermal regulation of vascular network bioengineering using a photopolymerizable methacrylated gelatin hydrogel. *Biomaterials*. 2013;34(28):6785–6796. https://doi.org/10.1016/j.biomaterials.2013.05.060.
44. Li BQ, Wang L, Xu F, et al. Hydrosoluble, UV-crosslinkable and injectable chitosan for patterned cell-laden microgel and rapid transdermal curing hydrogel *in vivo*. *ACTA Biomater*. 2015;22:59–69. https://doi.org/10.1016/j.actbio.2015.04.026.
45. Peng H, Ling J, Liu JZ, Zhu N, Ni XF, Shen ZQ. Controlled enzymatic degradation of poly(ε-caprolactone)-based copolymers in the presence of porcine pancreatic lipase. *Poly Degrad Stabil*. 2010;95(4):643–650. https://doi.org/10.1016/j.polymdegradstab.2009.12.005.
46. Li SM, Espartero JL, Foch P, Vert M. Structural characterization and hydrolytic degradation of a Zn metal initiated copolymer of L-lactide and ε-caprolactone. *J Biomater Sci*. 1996;8(3):165–187. https://doi.org/10.1163/156856296×00237.
47. Li SM, Liu LJ, Garreau H, Vert M. Lipase-catalyzed biodegradation of poly(ε-caprolactone) blended with various polylactide-based polymers. *Biomacromolecules*. 2003;4(2):372–377. https://doi.org/10.1021/bm025748j.
48. Pitt CG, Hendren RW, Schindler A, Woodward SC. The enzymatic surface erosion of aliphatic polyesters. *J Control Rel*. 1984;1:3–14. https://doi.org/10.1016/0168-3659(84)90016-6.
49. Browning MB, Cereceres SN, Luong PT, Cosgriff-Hernandez EM, Hernandez EM. Determination of the *in vivo* degradation mechanism of PEGDA hydrogels. *J Biomedic Mater Res Part A*. 2014;102(12):4244–4251. https://doi.org/10.1002/jbm.a.35096.